Detonation simulations in supersonic flow under circumstances of injection and mixing

Wandong Zhao[a], Ralf Deiterding[b], Jianhan Liang[a,*], Xiaodong Cai[a,*], Xinxin Wang[a]

[a] *Science and Technology on Scramjet Laboratory, College of Aerospace Science and Engineering, National University of Defense Technology, Changsha 410073, China*
[b] *Aerodynamics and Flight Mechanics Research Group, University of Southampton, Boldrewood Innovation Campus, Southampton SO16 7QF, United Kingdom*

Abstract

The unsteady, reactive Navier-Stokes equations with a detailed chemical mechanism of 11 species and 27 steps were employed to simulate the mixing, flame acceleration and deflagration to detonation transition (DDT) triggered by transverse jet obstacles. Results show that multiple transverse jet obstacles ejecting into the chamber can be used to activate DDT. But the occurrence of DDT is tremendously difficult in a supersonic non-uniform mixture so that it required several groups of transverse jets with increasing stagnation pressure. The jets introduce flow turbulence and produce oblique and bow shock waves even in an inhomogeneous supersonic mixture. The DDT is enhanced by multiple explosion points that are generated by the intense shock wave focusing of the leading flame front. It is found that the partial detonation front decouples into shock and flame, which is mainly caused by the fuel deficiency, nevertheless the decoupled shock wave is strong enough to reignite the mixture to detonation conditions. The resulting transverse wave leads to further mixing and burning of the downstream non-equilibrium chemical reaction, resulting in a high combustion temperature and intense flow instabilities. Additionally, the axial and transverse gradients of the supersonic non-uniform mixture induce a highly dynamic behavior with sudden propagation speed increase and detonation front instabilities.

Keywords: Deflagration-to-detonation transition; Non-uniform supersonic mixture; Detonation propagation; Flame acceleration

---

*Corresponding author.
*Email: jhleon@vip.sina.com (**Jianhan Liang**);*
*Email: cai-chonger@hotmail.com (**Xiaodong Cai**)*

1. Introduction

Thanks to the high thermodynamic efficiency of detonation combustion, it has become a potential combustion model to enhance aerospace thrust performance [1]. Practical detonation-based engines will employ non-uniform mixtures with velocity, temperature, and species gradients. Hence, the current work presents a detailed study of the flame acceleration (FA), deflagration-to-detonation transition (DDT), and detonation propagation under the influence of supersonic injection and mixing conditions for an air-breathing detonation engine.

One of the essential issues for such engines is to obtain a robust detonation initiation. Most prior studies addressing activation of DDT have used fixed obstructions such as a wedge, orifice or Shchelkin spiral [2-5]. However, these approaches face vast challenges in the form of propulsion loss when the mixture has a high flow velocity [6], especially for an air-breathing detonation engine [7]. Therefore in recent years the transverse jet obstacle has been introduced to trigger DDT [8, 9], which is advantageous compared to the fixed obstructions as confirmed by many previous studies [10, 11]. While in most previous studies, the mixture has typically been considered at a steady and uniform state. In most real-world scenarios the mixture would be unevenly distributed, hence it is more challenging to predict the occurrence of the onset of detonation.

We have comprehensively investigated detonation initiation and DDT from transverse hot jets under uniform and premixed conditions [12-14]. There are few studies that evaluate transverse jets to shorten DDT time and length in non-uniform mixtures, and the setup of the jet arrangement, jet pressure, and the required number of jets are rarely reported. There have been some studies on FA [15, 16], DDT [17-19], and detonation propagation [20-22] in non-uniform mixtures with a concentration gradient using a smooth tube or solid-laden chamber. In contrast to homogeneous mixtures, it is revealed that detonation propagation has a more dynamical behavior because of the fuel-lean or fuel-rich impacts [21, 23]. Most prior works regarding non-uniform mixtures are associated with artificial distributions in the main flow and a linear concentration gradient in the transverse directions of the chamber so that the detonation propagation rarely leads to extinction.

For these reasons, the motivation of this investigation is to understand how to obtain the onset of detonation with a short run-up distance and length under the influence of transverse jets. Additionally, the detonation propagation characteristics and mechanisms in such an uneven hydrogen-air mixture are also revealed in detail. Here, we consider just one case of a supersonic non-uniform mixture, which is close to a practical detonation-based engine under supersonic flighting condition. The unsteady, reactive Navier-Stokes (N-S) equations are employed to carry out the mixing, FA, DDT, and detonation propagation in a two-dimensional (2D) combustion chamber. A high-resolution mesh with structured adaptive mesh refinement (AMR) technique is employed to numerically solve the FA and detonation propagation. The solver is implemented within the AMROC (Adaptive Mesh Refinement Object-oriented C++) framework and has been successfully applied to simulate FA, detonation propagation and supersonic combustion [12, 13]. The chemical reaction is modeled by a system of Arrhenius-type equations and uses 11 species 27 steps. We comprehensively study the processes and mechanisms of the successful and unsuccessful DDT and the subsequent dynamic detonation behaviors in the supersonic non-uniform mixture. Hence, the main novelty of this work is to evaluate the effect of the transverse jet on DDT and present a fundamental understanding of the mechanisms of detonation propagation in a highly inhomogeneous supersonic mixture by considering the fuel injection and air-fuel mixing processes.

2. Physical and numerical models

The schematic illustration of an air-breathing PDE engine configuration under supersonic injection and mixing processes and its boundary conditions is shown in Fig. 1, which is composed of two parts, including the inlet isolation section of $Li \times Ly$=180 × 20mm^2, where a shock wave (SW) is formed, and the combustion chamber of $Lc \times Ly$=800 × 20mm^2. A working flight condition at 1km altitude is considered in this study. The air is flowing into the chamber with temperature T=281.7K and pressure P=0.09MPa. The inflow is set at supersonic flight with Ma=1.5. Four transverse fuel jets are injected into the chamber with a pressure of 1.0Mpa, and the jet size equals 0.2mm, in order to maintain a global stoichiometric equivalence ratio (ER). The parameters S_1 and S_2 are taken as 20mm and 30mm, respectively. The non-uniform mixture is therefore generated in the downstream chamber, and the mixing time is set as t=0.84ms. After the mixing process, a pair of two half-circle hot spots (r=4mm) with slightly high energy (T=2500K and P=0.5MPa) is adopted to ignite the non-uniform mixture and to prevent flameout. A profile of half circle of the ignition kernel is widely employed in former DDT studies [3, 4, 11]; the alternative use of ignition by a pre-detonator needs further study. The spots are located in the upper and lower sides of the connection part. The impacting transverse jets are employed to stimulate FA, as plotted by the blue jet in Fig. 1. After the end of the mixing process, and to compare the effect of jet obstacles on the DDT, no transverse jet obstacle is considered as Case A, while two and four groups of jet obstacles with different jet pressures and operation times are utilized, corresponding to Cases B and C, respectively. The interval between jet and jet size are S_3=90mm and d=2mm, respectively. The first, second, third and fourth groups of jet obstacles are operated successively, with a time period of 1.1-1.3ms, 1.15-1.4ms, 1.3-1.5ms and 1.4-1.6ms, respectively. The pressure of the first and second groups of jet obstacles in Cases B and C is P=0.6MPa. The pressure of the third and fourth groups of jet obstacles in Case C is P=1.2MPa. Note

that the fuel jets are hydrogen, whereas the jet obstacles are the premixed mixture. All jets have pressure inlet boundary condition (BC). The velocity inlet BC is specified in the left side of the computation domain, whereas a no-slip adiabatic wall is assumed when the inlet valve is closed after the ignition has ceased due to the PDE operation. The outlet flow BC is set on the right side of the computational domain.

The unsteady, reactive 2D N-S equations were employed to simulate the flow and combustion processes; a detailed description of the governing equations can be found in Ref. [13]. A hybrid Roe-HLL Riemann solver was utilized to discretize the upwind fluxes to avoid unphysical total density and internal energy near vacuum due to the Roe linearization. The MUSCL scheme together with Minmod limiter was applied for reconstruction. The diffusion terms are discretized by conservative central differences. In terms of chemical reaction source, the Godunov splitting with first-order accuracy was used [24]. A semi-implicit generalized Runge-Kutta scheme with fourth-order accuracy was adopted for the integration of the chemical kinetics [25]. A dynamic time step was assumed under a Courant-Friedrichs-Lewy (CFL) number of 0.18. A detailed chemical reaction mechanism proposed by Burke et al. [26] was utilized to model the reaction of deflagration and detonation flames. The thermodynamic properties and transport parameters were determined by the CHEMKIN package.

The initial grid was set as 4900 × 100 cells, generating an equal size mesh in both x and y directions of dx=dy=0.2mm. The governing equations were solved in AMROC utilizing AMR. A mesh resolution test for DDT simulation has been conducted before this study. From two to four additional levels refined by a factor 2 were used, denoted by L3 (2,2), L4 (2, 2, 2), and L5 (2, 2, 2, 2), yielding highest refined mesh sizes of 0.05mm, 0.025mm, 0.0125mm, respectively. It is found that there is a 2.36% deviation of DDT time in the case of L4 compared to L5 and the DDT distances in the cases of L4 and L5 are almost the same. As such, the fourth level L4 configuration was utilized for the current simulation, which would correspond to 31.36 million cells when using a uniform mesh. The cases were run on the Tianhe-1 supercomputer, where 660 cores were adopted to perform the computations, and one case took about 216000 cpu × h.

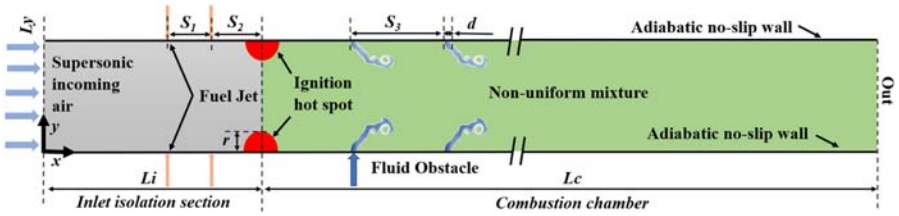

Fig. 1. Schematic illustration of the combustion configuration and boundary conditions with injection and mixing conditions.

3. Results and discussion

3.1. The mixing process in a supersonic flow

The H_2 mass faction contour at t=0.8ms and the mixture fraction (Z) distributions along the horizontal and transverse directions before the mixture ignition are given by Figs. 2(a), 2(b) and 2(c), respectively. Unless specifically described, all units on x-axes in this study's contours are centimeters. In Fig. 2(a), the mixture is mainly generated by the Kelvin-Helmholtz (K-H) instability, producing a lot of vortexes. Thus, a dramatically uneven distribution of H_2 is formed, especially in the downstream tube, and in some regions, there does not exist any H_2 anymore, while the uniformity of mixture increases in the downstream tube. The mass fraction is decreased along the axial direction and has a high amplitude fluctuation, as seen in the variations of Fig. 2(b), whereas in the downstream and middle regions, more homogenous mixture distributions are presented, as shown in the circle A in Fig. 2(c). Note how these regions are close to stoichiometric conditions (Z_{st}). Additionally, the mixing uniformity in the upper and lower parts also increases with the mixture moving downstream thanks to the flow instabilities and turbulent diffusion influences. In all, the hydrogen-air mixture in the combustion chamber is far away from the Z_{st} state.

3.2. Flame acceleration and DDT

The snapshots of the FA and DDT processes, rendered by temperature contours as a function of time, are given in Fig. 3 for Case C with four groups of transverse jets. After the mixture is ignited by two hot spots in the upper and lower walls, crumbled flames are introduced due to the K-H instability. They move and spread downstream under the influence of the supersonic main flow, as seen in Fig. 3(b). The two transverse jets are injected into the chamber, and they are deflected remarkably because of the main flow, as seen in Figs. 3(b-d), introducing vast mushroom vortices and turbulent perturbances. These are also confirmed by prior studies in FA triggered by transverse jets [11, 27, 28]. Although the surface area of the propagating flame is elongated dramatically owing to the intense turbulence, low temperature of the combustion products (see rectangle A) is formed as the detrimental mixing uniformity appears in the downstream tube, as revealed by Fig. 2(a).

A preheated zone ahead of the transverse jet is formed by the oblique and bow shock when the second group of transverse jets is injected into the chamber, as seen in Fig. 3(c). Flame-turbulence (F-T) interactions and turbulence vortices generated by the transverse jet

also take place in Figs. 3(c-d), and these features increase the flame surface area and mixing uniformity.

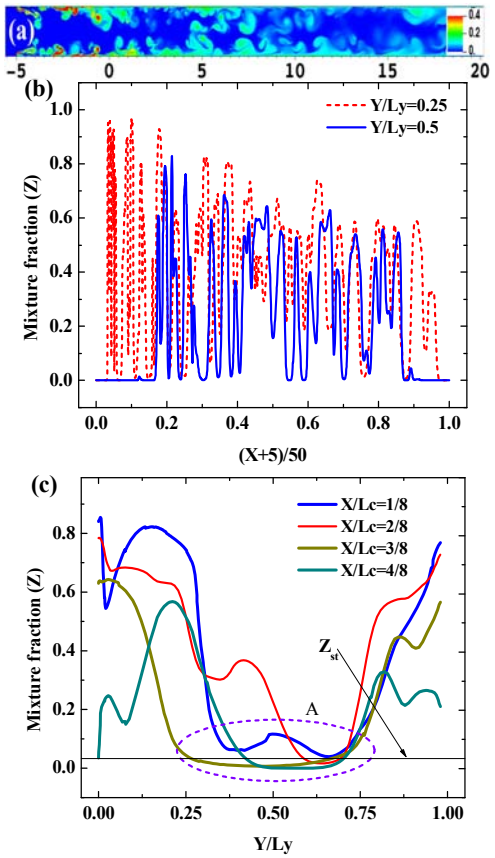

Fig. 2. The (a) H_2 mass fraction contour at t= 0.8ms and the mixture fraction variations along (b) main flow and (c) transverse directions at the end of the mixing process.

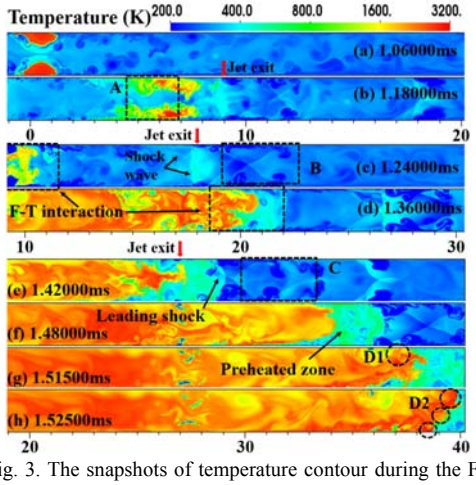

Fig. 3. The snapshots of temperature contour during the FA and DDT processes in the combustion chamber with four transverse jets (Case C).

As such, the combustion intensity is augmented so that the flame temperature is increasing from 1700K to 2400K, as seen in Fig. 3(d), feeding back to the flame propagating speed as high as 1000m/s. A leading SW is therefore produced by the intense FA, as demonstrated by Figs. 3(e-f). A higher penetration depth is found in the third group transverse jet with high jet pressure, as depicted by rectangle C. Due to the moment ratio between the transverse jet and main flow, the flow area of the main flow effectively decreases, hence, a high blockage ratio is formed within the tube compared to the first two sets of jets. These contribute to the high turbulent penetration in the downstream tube and form a stronger SW that interacts with the leading SW, leading to a highly preheated zone when the leading SW propagates into the unburned mixture, as seen in Fig. 3(f). This forms a condition for DDT, and it also contributes to the burning rate increase. Subsequently, a local explosion point has occurred on the upper wall, as seen in the series circles from D1 to D2 during the shock-flame complex region [4, 29]. Furthermore, more explosion points have occurred within the leading flame tips in Fig. 3(h). Therefore, the onset of detonation is activated in the supersonic non-uniform mixture under the influence of several groups of transverse jets.

3.3. Mechanisms of DDT

In order to reveal the process and mechanism of the DDT in the non-uniform mixture in Case C, the temperature and the corresponding pressure variations around DDT are given in Fig. 4. As shown, a small fingertip flame in the preheated zone ahead of the leading SW hits the upper wall, and a high-pressure spot with high value P=4.6MPa is formed in the same region due to the sustainable shock waves that impact and focus around the flame tip. As a result, a local explosion appears on the upper wall, as presented in circle B1, which also generates a stronger SW that propagates around as seen in Fig. 4(b2). However, the explosion point cannot be developed into a detonation wave (DW) because of the shortage of mixture downstream. Nevertheless, the intense SW still propagates forward, and the detonation initiation appears when it spreads to the regions having new mixture, as noted in circle B4. Thus, the post-shock pressure is elevated to P=9.0MPa due to the overdriven detonation. Moreover, as several shock waves focus and impact into the flame tip, more explosion points are further produced, as shown in circles C1 and D1, generating a high-pressure spot with P=10.5MPa and T=2850K. Such features are consistent with prior research on fast flames [30, 31]. These explosive spots further develop into DW in the downstream tube. Therefore, the supersonic non-uniform mixture also experiences a DDT process via the Zeldovich gradient mechanism [3, 32].

Figure. 5 plots the records of the variations of the flame front and the corresponding flame front propagation velocity for Cases A, B and C, respectively. As presented, the FA in all cases can be divided into four stages. Stage I: ignition process, a high propagation

velocity is generated at the initial hot spot ignition but decreases promptly. Stage II in Case A has a rapidly increasing velocity under the effect of main flow effect. While in Cases B and C, the transverse jet injects into the chamber, generating a blockage ratio and high-pressure regions ahead of the flame front. Therefore, stage II is a constant propagation velocity process, where the flame propagating in the tube that has a lower temperature as discussed above. Stage III is the FA process caused by the increasing flame surface areas. In this stage, the flame propagation velocity can be accelerated to about half CJ value as 1100m/s. Whereas the required time in Case A is around 3 times that in Case B and Case C, therefore, the multiple transverse jets have a high efficiency to increase the flame propagation speed.

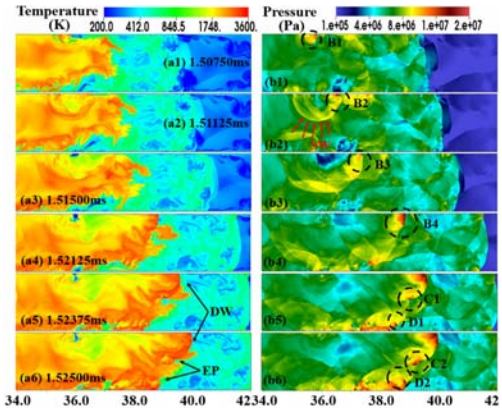

Fig. 4. The snapshots of temperature (left) and pressure (right) contours during DDT process in Case C. DW-detonation wave, EP-explosive point, SW-shock wave.

In the IV stage of Case A and Case B, as shown in Figs. 5(a) and 5(b), the combustion process in the supersonic mixture cannot be developed to detonation combustion. Instead, deflagration combustion results from the weak leading SW in Case A and less flow blockage ratio provided by the transverse jet in Case B. The leading SW is too weak in Case A, resulting in a low post-shock temperature. Although a remarkable leading SW in front of the flame tip is formed, the distance between the flame tip and leading SW (L_{fs}) [33] is gradually increasing, resulting in a failure of DDT in Case B. On the contrary, as more transverse jets are injected into the downstream chamber in Case C, it generates more turbulent flows and vortexes, as well as providing oblique and bow shock waves, which enhance the intensity of the leading SW that further increases the post-shock temperature and elevates the burning rate. As such, a transition to DDT occurs, as indicated by the steeper velocity curve in Fig. 5(c). Then, the overdriven detonation decays, but there is a high fluctuation of the propagation speed in the supersonic non-uniform mixture in the VI stage of Case C.

In general, these global phenomena are qualitatively similar to prior studies of the FA and DDT processes [34] that occur in the solid-laden combustion tube filled with premixed hydrogen-air mixture. However, the activation of the onset detonation will become more difficult and complicated due to the poor mixture uniformity, especially in a smooth chamber. An intense and shorter distance of L_{fs} has a dramatical influence on the detonation initiation.

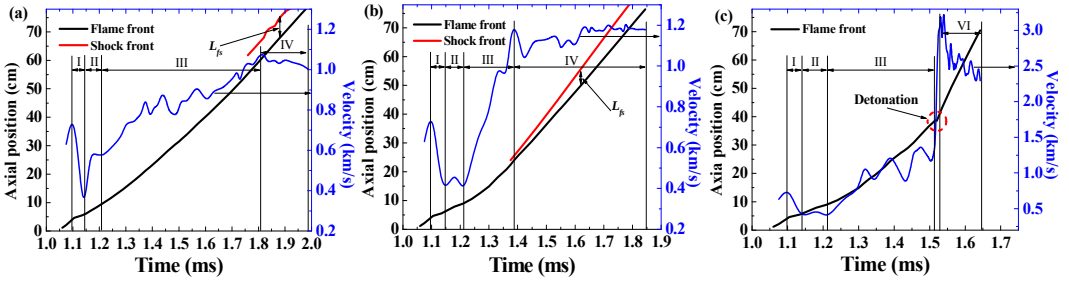

Fig. 5. The axial position of the flame and the leading SW, and the corresponding flame propagation velocity versus time in (a) Case A (no jet), (b) Case B, two groups of jet, and (c) Case C, four groups of jet. The blue line represents the propagation velocity.

3.4. Detonation propagation in supersonic non-uniform mixture

As noted above in Fig. 5(c), a significantly fluctuating velocity is found at the detonation stage. As a consequence, Fig. 6 provides snapshots of the temperature contours during the detonation propagation stage. Of note, the smooth overdriven DW is formed before the detonation tip catches up with the leading SW owing to the reduced ratio between the von Neumann temperature and the activation temperature [31, 35], while an irregular detonation front is formed as shown in boxes A and B. This is attributed to the extremely inhomogeneous mixture that does not have enough time to equilibrate before the DW approaches, see box C. Moreover, the transverse wave can be clearly noted in Figs. 6(c-d). There is a higher temperature region in the partial combustion products, which contributes to the further combustion due to the unburned material that still exists in the downstream flame. Note that a lot of turbulent vortices and non-uniform temperature contours are generated downstream, as seen in circle E due to the Richtmyer-Meshkov instability and the uneven distribution of the combustion products [21]. Hence,

the transverse wave further results in the mixing and burning of the downstream non-equilibrium chemical reaction.

For further revealing the mechanisms of DW propagation in detail, Fig. 7 provides the temperature, ER, pressure and product contours as a function of time. A clear evolution of the triple point can be observed, as seen in the series of circles A1-A5, in which the DW is decoupled into flame and SW, and the intensity of SW in the circle A3 and A4 is strengthened as shown by Figs. 7(c3) and 7(c4). Further, the intense SW is transferred to DW, as highlighted by the circle A5 of Fig. 7(a5), where the Mach stem with high temperature is generated in Fig. 7(c5). All the complicated features of the detonation front are the result of the variations in the non-uniform mixture, as seen by the series of the ER contours in Figs. 7(b1-b5). In the products regions, the ER maps are composed of gray (ϕ =0) and brown ($\phi = \infty$), indicating that the fuel and oxidizer has been depleted [18], underscoring that there is still a large amount of residual fuel in the combustion downstream. Initially, a dramatically uneven distribution of ER is formed ahead of the detonation front, where the boxes B1, B2, and B3 have lower ($\phi \approx$ 0-0.3), suitable ($\phi \approx$ 1.0) and higher ($\phi \approx$ 1.6) ER. As a result, when the DW approaches the fuel-lean region, it decouples into flame and SW as discussed above, while the DW can be re-ignited again when the strong SW approaches into a suitable ER region, as seen in box B4. A new decoupled region is generated when the DW crosses the B5 region. Hence, non-uniform combustion products are formed in the downstream tube and flame front. Lower value distributions are formed when the DW is decoupled. A region with a high product value that represents the detonation re-initiation is formed.

These detonation propagation characteristics can be quantitatively analyzed by the records of the temperature and pressure variations in Fig. 8. As seen in the grey line A, formed by the maximum temperature of the flame front, the peak temperature reduces from 3255K to 1800K during the detonation extinction process. Next, the pressure further augments from 3.0MPa to 4.3MPa at the pressure-augment stage as demonstrated by the violet line, while the detonation wave is further extinguished in the next stage, because it spreads to the fuel-lean regions, as demonstrated in Fig. 7(b5) at t=1.5675ms.

Figure 9 depicts the triple point trajectory and the detonation front from t=1.58ms to t=1.6175ms, and the transient detonation propagation velocity is also superimposed on Fig. 9(b). Thanks to the inhomogeneous ER maps, as presented above, the detonation tip scenarios are quantitatively different from the homogenous hydrogen-air mixture. A strong and irregular triple point trajectory is formed within the chamber, and a new triple point trajectory is also generated in line A. These features are mainly attributed to the fuel-lean mixture that yields a more complicated trajectory so that the non-uniform mixture promotes cellular detonation instability [23, 36]. The vertical fuel deficit also leads to the curved detonation front. Meanwhile, the transient flame front propagation velocity has a higher fluctuation amplitude than the natural instability of DW from the upper to the lower wall, as shown in Fig. 9(b). It is also found that the detonation propagation velocity is suddenly increased to a stage with high average velocity magnitude, which is similar to the former study in the concentration gradient mixture [21]. This is mainly caused by the dramatic influence of the transverse ER gradient, which prompts the detonation propagation instability.

In summary, the supersonic non-uniform mixture results in extremely complicated DW propagation characteristics including the irregular triple-point, a highly fluctuating detonation propagation velocity, stronger SW, and non-equilibrium chemical reaction in the fuel deficiency regions with transverse and axial-direction ER gradient. The sudden changes of the ER gradient mixture are the main reason for these phenomena, but it enhances the propagation instabilities of the DW

4. Conclusions

The processes for mixing, ignition, FA, DDT, and detonation propagation under supersonic injection and mixing conditions trigged by jet obstacles were numerically studied by solving the unsteady N-S equations with a detailed chemical reactive mechanism and AMR technique. The main conclusions are as follows:

1. The transverse jet obstacle can be employed to activate DDT in a supersonic non-uniform mixture because it introduces intense turbulent flow and vortices and provides a suitable blockage ratio that generates oblique and bow shock waves, forming an intense leading SW, and therefore it promotes the FA. However, sufficient numbers of transverse jet groups with an increased stagnation pressure are required.
2. A DDT is extremely difficult in a non-uniform mixture. The leading SW should be stronger to create a transition condition; conversely, the transition will fail when there is an increasing length of L_{fs}. The DDT mechanism is attributed to the multiple explosion points that develop to DW through the Zeldovich gradient mechanism.
3. The fuel deficiency is the main reason to generate a local detonation extinction that decouples into separated flame and shock. Its intense shock can be further reignited to a DW when it propagates to a suitable ER mixture. Such features mainly result in a dramatically irregular tiple point trajectory, accompanied by a new generation of triple point and an unstable detonation front with high fluctuation propagation and suddenly increased velocities when the DW propagates from extreme fuel-lean to suitable ER regions.
4. Thanks to the significantly perturbed mixture homogeneity, the unburned H_2 and non-equilibrium chemical reaction is further spread to the downstream chamber and hence promotes the downstream temperature of combustion products and the intensity of flow vortices.

Although this study is in 2D, it still gives a good insight on how the jet affects the DDT, especially under the injection and mixing conditions. Further on, the 2D simulations also allow many preliminary qualitative conclusions. A 2D jet in crossflow would have a high blockage ratio, but the diffusion and disturbance effects in a 3D jet would be higher than in the 2D simulation. The effect of the 3D jet on the FA and DDT in the supersonic non-uniform mixture should be studied in further work.

Acknowledgements

This work was supported by the National Natural Science Foundation of China (Nos. 11925207 and 91741205) and the China Scholarship Council (No. 202106110005).

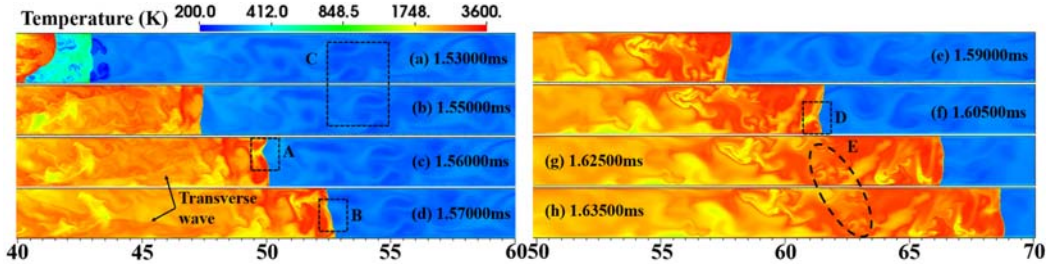

Fig. 6. The temperature evolution during the detonation wave propagation in the non-uniform supersonic mixture.

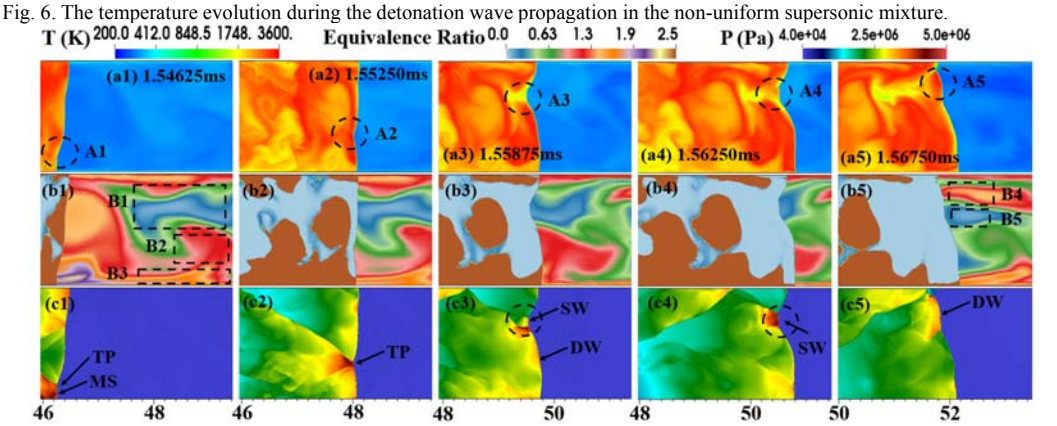

Fig. 7. The time evolution of (upper-row) temperature, (middle-row) equivalence ratio, and (lower-row) pressure contours when detonation wave passing remarkable fuel-lean and fuel-rich mixture.TP- triple-point, MS-Mach stem.

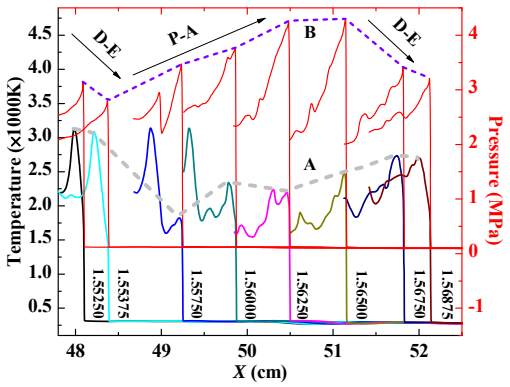

Fig. 8. Transient temperature and pressure variations along x-direction in the region of Y/Ly=0.675. Detonation extinction (D-E), pressure augmentation (P-A).

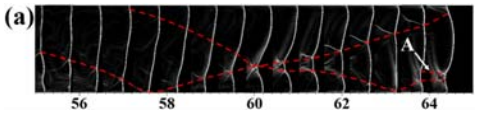

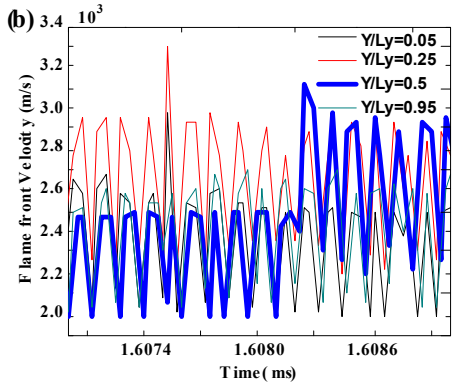

Fig. 9. (a) The triple point evolution and (b) flame front propagation velocity versus time.

Reference

[1] G.D. Roy, S.M. Frolov, A.A. Borisov, D.W. Netzer, Pulse detonation propulsion: challenges, current status, and future perspective, Prog. Energy Combust. Sci. 30 (2004) 545-672.

[2] G. Ciccarelli, S. Dorofeev, Flame acceleration and transition to detonation in ducts, Prog. Energy Combust. Sci. 34 (2008) 499-550.
[3] E.S. Oran, G. Chamberlain, A. Pekalski, Mechanisms and occurrence of detonations in vapor cloud explosions, Prog. Energy Combust. Sci. 77 (2020) 100804.
[4] V.N. Gamezo, C.L. Bachman, E.S. Oran, Flame acceleration and DDT in large-scale obstructed channels filled with methane-air mixtures, Proc. Combust. Inst. 38 (2021) 3521-3528.
[5] H. Xiao, E.S. Oran, Flame acceleration and deflagration-to-detonation transition in hydrogen-air mixture in a channel with an array of obstacles of different shapes, Combust. Flame 220 (2020) 378-393.
[6] M. Cooper, S. Jackson, J. Austin, E. Wintenberger, J. Shepherd, Direct experimental impulse measurements for detonations and deflagrations, J. Propul. Power 18 (2002) 1033-1041.
[7] S.M. Frolov, V.S. Aksenov, V.S. Ivanov, I.O. Shamshin, A.E. Zangiev, Air-breathing pulsed detonation thrust module: Numerical simulations and firing tests, Aerosp. Sci. Technol. 89 (2019) 275-287.
[8] K.A. Ahmed, D.J. Forliti, Fluidic Flame Stabilization in a Planar Combustor Using a Transverse Slot Jet, AIAA J. 47 (2009) 2770-2775.
[9] B. Knox, D. Forliti, C. Stevens, J. Hoke, F. Schauer, A Comparison of Fluidic and Physical Obstacles for Deflagration-to-Detonation Transition, 49th AIAA aerospace sciences meeting including the new horizons forum and aerospace exposition, Orlando, Florida, (2011) 587.
[10] J.P. McGarry, K.A. Ahmed, Flame–turbulence interaction of laminar premixed deflagrated flames, Combust. Flame 176 (2017) 439-450.
[11] H. Peng, Y. Huang, R. Deiterding, Z. Luan, F. Xing, Y. You, Effects of jet in crossflow on flame acceleration and deflagration to detonation transition in methane–oxygen mixture, Combust. Flame 198 (2018) 69-80.
[12] X. Cai, R. Deiterding, J. Liang, Y. Mahmoudi, Adaptive simulations of viscous detonations initiated by a hot jet using a high-order hybrid WENO–CD scheme, Proc. Combust. Inst. 36 (2017) 2725-2733.
[13] X. Cai, J. Liang, R. Deiterding, Y. Mahmoudi Larimi, M.-B. Sun, Experimental and numerical investigations on propagating modes of detonations: Detonation wave/boundary layer interaction, Combust. Flame 190 (2018) 201-215.
[14] X. Cai, R. Deiterding, J. Liang, Y. Mahmoudi Larimi, Mechanism of detonation stabilization in supersonic model combustor, J. Fluid Mech. 910 (2020) A40.
[15] K. Vollmer, F. Ettner, T. Sattelmayer, Deflagration-To-detonation Transition in Hydrogen-Air Mixtures with a Concentration Gradient, Combust. Sci. Technol. 184 (2012) 1903-1905.
[16] M.H. Shamsadin Saeid, J. Khadem, S. Emami, Numerical investigation of the mechanism behind the deflagration to detonation transition in homogeneous and inhomogeneous mixtures of H2-air in an obstructed channel, Int. J. Hydrogen Energy 46 (2021) 21657-21671.
[17] K. Ishii, M. Kojima, Behavior of detonation propagation in mixtures with concentration gradients, Shock Waves 17 (2007) 95-102.
[18] W. Zheng, C.R. Kaplan, R.W. Houim, E.S. Oran, Flame acceleration and transition to detonation: Effects of a composition gradient in a mixture of methane and air, Proc. Combust. Inst. 37 (2019) 3521-3528.
[19] F. Ettner, K.G. Vollmer, T. Sattelmayer, Mach reflection in detonations propagating through a gas with a concentration gradient, Shock Waves 23 (2013) 201-206.
[20] X. Mi, A. Higgins, H.D. Ng, C. Kiyanda, N. Nikiforakis, Propagation of gaseous detonation waves in a spatially inhomogeneous reactive medium, Phys. Rev. Fluids 2 (2017) 053201.
[21] W. Han, C. Wang, C.K. Law, Role of transversal concentration gradient in detonation propagation, J. Fluid Mech. 865 (2019) 602-649.
[22] K. Iwata, O. Imamura, K. Akihama, H. Yamasaki, S. Nakaya, M. Tsue, Numerical study of self-sustained oblique detonation in a non-uniform mixture, Proc. Combust. Inst. 38 (2021) 3651-3659.
[23] S. Boulal, P. Vidal, R. Zitoun, Experimental investigation of detonation quenching in non-uniform compositions, Combust. Flame 172 (2016) 222-233.
[24] R. Deiterding, Parallel adaptive simulation of multi-dimensional detonation structures, PhD thesis, Brandenburg University of Technology, Cottbus, Brandenburg, 2003.
[25] P. Kaps, P. Rentrop, Generalized Runge-Kutta methods of order four with stepsize control for stiff ordinary differential equations, Numerische Mathematik 33 (1979) 55-68.
[26] M. Burke, M. Chaos, Y. Ju, F. Dryer, S. Klippenstein, Comprehensive H2/O2 kinetic model for high - pressure combustion, Int. J. Chem. Kinet. 44 (2012) 444-474.
[27] W. Zhao, J. Liang, R. Deiterding, X. Cai, X. Wang, Effect of transverse jet position on flame propagation regime, Phys. Fluids 33 (2021) 091704.
[28] J. Cheng, B. Zhang, H. Dick Ng, H. Liu, F. Wang, Effects of inert gas jet on the transition from deflagration to detonation in a stoichiometric methane-oxygen mixture, Fuel 285 (2021) 119237.
[29] J.H.S. Lee, R. Knystautas, C.K. Chan, Turbulent flame propagation in obstacle-filled tubes, Sym. Combust. 20 (1985) 1663-1672.
[30] M.F. Ivanov, A.D. Kiverin, M.A. Liberman, Hydrogen-oxygen flame acceleration and transition to detonation in channels with no-slip walls for a detailed chemical reaction model, Phys. Rev. E 83 (2011) 056313.
[31] G.B. Goodwin, R.W. Houim, E.S. Oran, Effect of decreasing blockage ratio on DDT in small channels with obstacles, Combust. Flame 173 (2016) 16-26.
[32] Y.B. Zel'Dovich, V.B. Librovich, G.M. Makhviladze, G.I. Sivashinsky, On the development of detonation in a non-uniformly preheated gas, Astronaut. Acta 15 (1970) 313-321.
[33] G.B. Goodwin, R.W. Houim, E.S. Oran, Shock transition to detonation in channels with obstacles, Proc. Combust. Inst. 36 (2017) 2717-2724.
[34] D.A. Kessler, V.N. Gamezo, E.S. Oran, Simulations of flame acceleration and deflagration-to-detonation transitions in methane-air systems, Combust. Flame 157 (2010) 2063-2077.
[35] V.N. Gamezo, T. Ogawa, E.S. Oran, Flame acceleration and DDT in channels with obstacles: Effect of obstacle spacing, Combust. Flame 155 (2008) 302-315.
[36] L.R. Boeck, F.M. Berger, J. Hasslberger, T. Sattelmayer, Detonation propagation in hydrogen–air mixtures with transverse concentration gradients, Shock Waves 26 (2016) 181-192.